

Berry curvature and spin-one color superconductivity

Noriyuki Sogabe^{1,2} and Yi Yin^{3,4}

¹*Department of Physics, University of Illinois, Chicago, Illinois 60607, USA*

²*Laboratory for Quantum Theory at the Extremes, University of Illinois, Chicago, Illinois 60607, USA*

³*School of Science and Engineering, The Chinese University of Hong Kong, Shenzhen, Guangdong, 518172, China*

⁴*Quark Matter Research Center, Institute of Modern Physics, Chinese Academy of Sciences, Lanzhou 730000, China*
(Dated: November 13, 2024)

We study the Berry curvature and topological aspects of a spin-one color superconductor. In the ultra-relativistic limit, the ground state is the color-spin locking phase (CSL) with the pairing between quarks of opposite chirality. Li and Haldane show in Ref. [1] that for generic Cooper pairs formed by Weyl fermions that carry opposite chirality, the gap function must have topologically protected nodes. However, the CSL phase has been known as a fully gapped system and lacks any nodes within one-flavor Quantum Chromodynamics (QCD). We present a general formulation relating the total topological number associated with the nodal structure and the monopole charges of the Berry curvature, including the color structure of the pair quarks. In the CSL phase, the contribution from the chirality, which is assumed to lead to the nodes within the conventional argument, is canceled out by the novel color contribution. Moreover, this non-trivial color Berry structure is manifested through the presence of gapless quasi-particles that exhibit the “color” helicity ± 1 , resulting in total monopole charges of $\pm 3/2$ rather than $\pm 1/2$ of a single Weyl fermion.

Introduction.—In many-body systems involving chiral (Weyl) fermions, the Berry curvature associated with those particles leads to various interesting transport phenomena. One prominent example is the chiral magnetic effect (CME) where the current is generated along the magnetic field applied in the system [2, 3]. Recent theoretical developments have highlighted the profound connections between the Berry curvature of chiral fermions, CME and quantum anomaly [4–6]. The consequence of CME has been observed in Weyl and Dirac semimetals [7–10] and is still under study in the quark-gluon plasma [11]. Additionally, Berry curvature also induces the spin Hall effect [4, 12]. The analogous effect in QCD plasma [13, 14], along with various other novel spin effects [15–18], are under intensive investigation through heavy-ion collision experiments [19, 20].

Much less attention has been paid to the role of Berry curvature in QCD matter at high densities and low temperatures. In this regime, the color superconductivity (CSC) emerges, characterized by a condensate of quark Cooper pairs. At sufficiently high baryon number density, the ground state is a color-flavor locking (CFL) phase, which involves the pairing of three light quarks [21, 22]. At lower densities, pairing between single-flavor quarks is plausible for a certain range of baryon density [23–25]. Since the attractive one-gluon exchange interaction is color antisymmetric, the spins must be symmetric to have an overall antisymmetric pairing wave function. Thus, within the one-flavor QCD, spin-one CSC occurs. Due to the rich spin and color structure of the Cooper pairs, several possible phases arise, such as the polar, planar, A, and CSL phases. Additionally, the chirality of the pairs varies; they can form in the same chirality (longitudinal phase), opposite chirality (transverse phase), or a mixture of both. We

shall explore the connection between Berry curvature and spin-one CSC.

In the condensed matter literature [1, 26], the “pairing monopole charge,” $\Delta q_{\text{ch}} \equiv q_{\text{ch}} - q'_{\text{ch}}$ (“ch” refers to chirality) is introduced to characterize the Berry structure for the pairing state. Here, q_{ch} and q'_{ch} are the Berry monopole charges of the two Weyl fermions forming Cooper pairs, and $q_{\text{ch}}, q'_{\text{ch}} = 1/2$ and $-1/2$ correspond to the monopole charges for a single right-handed and left-handed chiral fermion, respectively. As shown in Ref. [1], the pairing monopole charges Δq_{ch} are connected to the sum of the topological number g around the gapless points (nodes) of the energy gap at the Fermi surface (F.S.) (see details below):

$$g = 2\Delta q_{\text{ch}}. \quad (1)$$

This relation predicts topologically protected nodes of the pairing gap function when $\Delta q_{\text{ch}} \neq 0$. The superconductivity (SC) with topological nodes has become a focus of extensive research [27, 28].

One may directly apply Eq. (1) to the spin-one CSC and conclude that its transverse phase must feature topological nodes. However, a puzzle arises: while some phases, such as polar and A phase, display point nodes, the energetically favored state, namely the transverse CSL phase, is found to be fully gapped [23, 25]. Why are the nodes absent in this phase despite $\Delta q_{\text{ch}} \neq 0$?

In this letter, we identify the missing element in the relation (1) that addresses the question—the color structure. The fact that pairing fermions carry additional quantum numbers, such as color in the case of QCD, significantly enriches the implications of non-zero Δq_{ch} . We incorporate the color contribution in the relation between the pairing monopole charge and the topological number associated with the nodes, g , see Eq. (10). By

doing so, we find that the conventional contribution Δq_{ch} is canceled by the novel color contribution and $g = 0$ in the fully gapped CSL phase. Moreover, we derive a surprising relation (23), among Δq_{ch} , g , and the color Berry monopole charges of the gapless excitations, which has not been discussed in the early condensed matter literature [1, 26]. This relation implies another scenario for the manifestation of the pairing monopole charges as topological gapless excitation, which must exist in the fully gapped CSL phase. We also demonstrate that even if the transverse and longitudinal phases share the same symmetry-breaking pattern, they can be distinguished based on their Berry structure and associated topology.

Berry flux and the topological nodes.—We shall show Eq. (10), which determines the relation between Berry flux of the pairing fermions and the sum of the topological number associated with the nodes, for a class of superconductors (SC) (including the spin-one CSC) described by the mean-field Hamiltonian in momentum space \mathbf{k} :

$$H = \int \frac{d^3\mathbf{k}}{(2\pi)^3} (\psi^\dagger, \psi'_c{}^\dagger) \begin{pmatrix} \mathcal{H}_0 & \Delta_0 M \\ \Delta_0 M^\dagger & \mathcal{H}'_{0c} \end{pmatrix} \begin{pmatrix} \psi \\ \psi'_c \end{pmatrix}, \quad (2)$$

where ψ and ψ' are fermionic fields that may carry additional quantum numbers beyond just spin, say color, and $\psi'_c(\mathbf{k}) = i\sigma_2\psi'^\dagger(-\mathbf{k})$ with Pauli matrices σ_i ($i = 1, 2, 3$) acting on the spinor space. The real value Δ_0 sets the overall magnitude of the gap (independent of \mathbf{k}), but its value is not relevant to the discussion that follows. For definiteness, we assume that there exist simultaneous eigenfunctions ϕ (ϕ') of free Hamiltonian \mathcal{H}_0 and MM^\dagger (\mathcal{H}'_{0c} and $M^\dagger M$), i.e.,

$$[MM^\dagger, \mathcal{H}_0] = 0, \quad [M^\dagger M, \mathcal{H}'_{0c}] = 0. \quad (3)$$

The Hermitian matrices MM^\dagger and $M^\dagger M$ share the same sets of eigenvalues λ , which are non-negative and might depend on \mathbf{k} . The eigenfunctions, ϕ_λ and ϕ'_λ , satisfy

$$MM^\dagger \phi_\lambda = \lambda \phi_\lambda, \quad M^\dagger M \phi'_\lambda = \lambda \phi'_\lambda. \quad (4)$$

The pairing states are formed by single-particle states with the same value of $\lambda \neq 0$, ϕ_λ and ϕ'_λ . If the degree of degeneracy at given λ is N_λ , we introduce a N_λ -dimension row vector $\Phi_\lambda \propto \{\phi_{\lambda,1}, \dots\}/\sqrt{N_\lambda}$ such that its components are orthonormal, i.e., $(\phi_{\lambda,m})^\dagger \phi_{\lambda,n} = \delta_{mn}$ where $m, n = 1, \dots, N_\lambda$ labels the degenerated eigenvectors and $\Phi^\dagger \Phi = 1$. The (non-Abelian) Berry connection ($N_\lambda \times N_\lambda$ matrix) is given by $\mathbf{A}_{\lambda,mn} = (-i\phi_{\lambda,m}^\dagger \nabla_{\mathbf{k}} \phi_{\lambda,n})/N_\lambda$ [29]. The row vector Φ'_λ associated with ϕ'_λ s and the corresponding Berry connection \mathbf{A}'_λ can be defined similarly. Under “rotation” (gauge transformation)

$$\Phi_\lambda \rightarrow \Phi_\lambda U_\lambda^\dagger, \quad \Phi'_\lambda \rightarrow U'_\lambda \Phi'_\lambda, \quad (5)$$

where U_λ and U'_λ are $U(N_\lambda)$ matrices, the “gauge connection” \mathbf{A}_λ and \mathbf{A}'_λ will transform as $\mathbf{A} \rightarrow U\mathbf{A}U^\dagger -$

$iU\nabla_{\mathbf{k}}U^\dagger$ and $\mathbf{A}' \rightarrow U'\mathbf{A}'U'^\dagger - iU'\nabla_{\mathbf{k}}U'^\dagger$. Here and hereafter, we omit the subscript λ and indices m, n when they are clear from the context. The single-particle Berry curvature now follows $F_{ij} = \partial_i A_j - \partial_j A_i + i[A_i, A_j]$. The Berry structure of a single-particle state is characterized by the flux of the trace of Berry magnetic field $B^i = \epsilon^{ijk} F_{jk}$ on the Fermi surface:

$$q = \frac{1}{4\pi} \iint_{\text{F.S.}} d\mathbf{S} \cdot \text{tr} \mathbf{B} = \frac{1}{4\pi} \iint_{\text{F.S.}} d\mathbf{S} \cdot (\nabla_{\mathbf{k}} \times \text{tr} \mathbf{A}), \quad (6)$$

and similarly for q' . Note that $2q = \pm 1$ is related to the first Chern number. A non-zero value of q indicates that Φ can not be defined globally on F.S. Without degeneracy, U and U' are simply $U(1)$ phase, and \mathbf{A} and \mathbf{A}' reduce to the Abelian Berry connection with q and q' representing those Berry monopole charges. We define the generalized “pairing monopole charge” as $\Delta q \equiv q - q'$.

Next, we connect the generalized “pairing monopole charge” to the topological number associated with the nodes of the projected gap function,

$$\tilde{M}_{mn}^\dagger \equiv \phi_m^\dagger M^\dagger \phi_n, \quad (7)$$

where we restored the m, n index for the degenerated vector space (at given λ). Recall that the topology of a superfluid is characterized by the circulation of superfluid velocity around defects where the superfluid is absent. The gauge-invariant combination of the phase gradient of the gap function and the gauge field in the real space gives the superfluid velocity. In analogous, we define the velocity field in the momentum space as

$$\mathbf{u} \equiv \nabla_{\mathbf{k}} \alpha - \text{tr}(\mathbf{A} - \mathbf{A}'), \quad (8)$$

where $\alpha = -i(\log \det \tilde{M}^\dagger)/N_\lambda$ is the phase of $\det \tilde{M}^\dagger$. It is clear that \mathbf{u} remains unchanged under the “gauge transformation” (5), as variations from $\nabla_{\mathbf{k}} \alpha$ and $\text{tr}(\mathbf{A} - \mathbf{A}')$ cancel out each other.

If there are nodes at $\hat{\mathbf{k}} \equiv \mathbf{k}/|\mathbf{k}| = \hat{\mathbf{k}}_{\text{node},N}$ ($N = 1, 2, \dots$) where the gap \tilde{M} (and λ) vanishes and α is ill-defined (see Fig. 1 (a)), we consider the circulation of \mathbf{u} along the infinitesimally small oriented loop (by the right-handed rule) C_N around $\hat{\mathbf{k}}_{\text{node},N}$. The node at $\hat{\mathbf{k}}_{\text{node},N}$ is termed “topological” when the circulation g_N is non-zero. Summing all circulations gives

$$g \equiv \frac{1}{2\pi} \sum_N \oint_{C_N} dt \cdot \mathbf{u} = \frac{-1}{2\pi} \iint_{\text{F.S.}} d\mathbf{S} \cdot (\nabla_{\mathbf{k}} \times \mathbf{u}), \quad (9)$$

where we have reversed the loop C_N and employed the Stokes theorem. Away from the nodes, $\nabla_{\mathbf{k}} \times \nabla_{\mathbf{k}} \alpha$ vanishes, and the “vorticity” in momentum space $\nabla_{\mathbf{k}} \times \mathbf{u}$ coincides with the tracing of the pairing Berry flux $-\nabla_{\mathbf{k}} \times (\mathbf{A} - \mathbf{A}')$ using (8). Thus, we find

$$g = 2\Delta q = 2(q - q'). \quad (10)$$

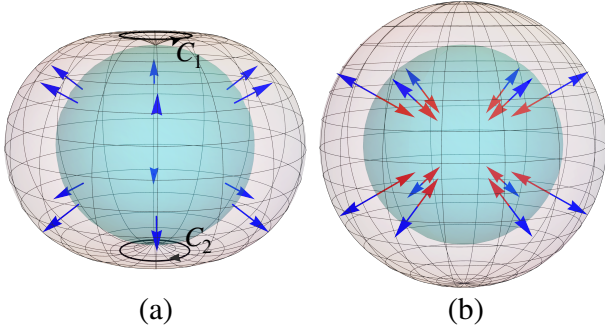


FIG. 1. Schematic representation of the energy eigenvalue $\sqrt{k^2 + \lambda(\hat{\mathbf{k}}) \Delta_0^2}$ around the F.S. for the transverse phase (the opposite chirality pairing) of spin-one CSC. The blue and red arrows illustrate the pairing of Berry flux from the chirality (spin) and color contributions, respectively. (a) The polar phase where the gap closes at the nodes at the north pole $\hat{\mathbf{k}}_{\text{node},1} = \hat{\mathbf{k}}_z$ and the south pole $\hat{\mathbf{k}}_{\text{node},2} = -\hat{\mathbf{k}}_z$. There is no color contribution to the pairing Berry flux. (b) CSL phase where the system is fully gapped. The pairing Berry flux from the color cancels that of the chirality.

The relation (10) generalizes the early one (1) and is new in literature to our knowledge. It tells us that total circulation g is determined not by Δq_{ch} but by Δq , which incorporates contributions to the pairing Berry flux from additional quantum numbers. This generalization allows us to analyze the novel topological aspects of spin-one CSC. We will demonstrate how Δq differs from Δq_{ch} in this particular example, in Eq. (18).

Spin-one CSC.—We begin by examining the pairing between quarks with opposite chirality (transverse phase) in light of relation (10). We concentrate on the right-handed quark ψ_{R} and left-handed quark ψ_{cL} (RL sector) pairing, as it decouples from the one between ψ_{L} and ψ_{cR} (LR sector) [23, 25]. The reduced Hamiltonian takes the form (2) with $\mathcal{H}_0 = \boldsymbol{\sigma} \cdot \mathbf{k} - \mu$ and $\mathcal{H}'_{0c} = -\mathcal{H}_0(-\mathbf{k})$ where μ represents chemical potential and the gap matrix M is described by

$$M = (P_+ \sigma_i^\perp) \Delta_{ia} J_a. \quad (11)$$

Here $(J_a)_{bc} = -i\epsilon_{abc}$ are the anti-symmetric color matrix with a and b denoting color index and ϵ_{abc} being the epsilon tensor. The spin matrix $\sigma_i^\perp = (\delta_{ij} - \hat{k}_i \hat{k}_j) \sigma_j$ is transverse to $\hat{\mathbf{k}}$ (hence the name “transverse” phase). We shall first derive results for general three-by-three matrix Δ_{ia} and will specify its components later (see Table I). The gap matrix M introduced in Eq. (11) satisfies Eq. (3), so the relation (10) is applicable. Additionally, Eq. (3) implies that the eigenfunctions of MM^\dagger and $M^\dagger M$ can possess definite helicity. With the helicity projection matrix $P_+ = (1 + \boldsymbol{\sigma} \cdot \hat{\mathbf{k}})/2$ appearing in M , we can show that, $M\xi_{\text{R}} = 0$ and $M^\dagger\xi_{\text{L}} = 0$, for normalized right-handed and left-handed spinors ξ_{R} and ξ_{L} , respectively. This highlights that Eq. (11) describes the RL sector. Noting

M in CSC is proportional to the director product of color and spin matrices, we now write the modes of interest as follows:

$$\phi_{\text{R}}(\hat{\mathbf{k}}) = c(\hat{\mathbf{k}}) \otimes \xi_{\text{R}}(\hat{\mathbf{k}}), \quad \phi'_{\text{L}}(\hat{\mathbf{k}}) = c'(\hat{\mathbf{k}}) \otimes \xi_{\text{L}}(\hat{\mathbf{k}}), \quad (12)$$

where c and c' are three-vectors in the color space with the normalization $\mathbf{c}^* \cdot \mathbf{c} = 1$. ϕ_{R} and ϕ'_{L} can be degenerated.

To determine c and c' , we substitute Eqs. (11) and (12) into Eq. (4). First, we observe

$$(P_+ \boldsymbol{\sigma}_\perp) \xi_{\text{L}} = \mathbf{l}_- \xi_{\text{R}}, \quad (P_+ \boldsymbol{\sigma}_\perp)^\dagger \xi_{\text{R}} = \mathbf{l}_+ \xi_{\text{L}}, \quad (13)$$

where the explicit expression for \mathbf{l}_\pm depends on the choice of $\xi_{\text{R,L}}$ (see Eq. (20) below). Interestingly, \mathbf{l}_\pm coincide with the eigenstate of the photon helicity operator $\mathbf{S} \cdot \hat{\mathbf{k}}$ with the eigenvalue ± 1 where $(S_i)_{jk} = -i\epsilon_{ijk}$ is the generator of SO(3) spatial rotation [30] (see also Ref. [31]). We denote $\mathbf{l}_0 = \hat{\mathbf{k}}$ as the helicity zero state for completeness.

Now Eq. (4) reduces to the eigenvalue problem in the color space:

$$NN^\dagger c = \lambda c, \quad N^\dagger N c' = \lambda c' \quad (14)$$

where the color matrix N is given by

$$N \equiv \xi_{\text{R}}^\dagger M \xi_{\text{L}} = \mathbf{n} \cdot \mathbf{J}, \quad n_a = (l_-)_i \Delta_{ia}. \quad (15)$$

Note also that we label the color vector by c_m at given λ if there is a N_λ -fold degeneracy. Using the definition of \mathbf{J} , we explicitly have,

$$(NN^\dagger)_{ab} = (\mathbf{n} \cdot \mathbf{n}^*) \delta_{ab} - n_a^* n_b. \quad (16)$$

where $n_a = \delta_{ai} n_i$ is a three-vector in color space. Eq. (16) immediately tells us that if color vector c_1 and c_2 are 1) orthonormal vectors in color space, e.g., $c_1^* \cdot c_2 = 0$ and 2) orthogonal to n_a^* , i.e., $c_1^* \cdot n^* = 0$ and $c_2^* \cdot n^* = 0$, c_1 and c_2 are degenerate non-zero modes of NN^\dagger with eigenvalue $\lambda = \mathbf{n} \cdot \mathbf{n}^*$.

The Non-Abelian Berry connection of the modes (12) becomes

$$\mathbf{A}_{mn} = \frac{1}{N_\lambda} (\mathbf{A}_{\text{co},mn} + \delta_{mn} \mathbf{A}_{\text{R}}), \quad (17a)$$

$$\mathbf{A}'_{mn} = \frac{1}{N_\lambda} (\mathbf{A}'_{\text{co},mn} + \delta_{mn} \mathbf{A}_{\text{L}}), \quad (17b)$$

where $\mathbf{A}_{\text{co},mn} = -ic_m^\dagger \nabla_{\mathbf{k}} c_n$ represent the “color contribution” to the Berry gauge field. Since the modes (12) are written in a direct product of the chirality and color contributions, the generalized “pairing monopole charge,” Δq , can also be separated into these spaces,

$$\Delta q = \Delta q_{\text{ch}} + \Delta q_{\text{co}}, \quad \Delta q_{\text{co}} \equiv q_{\text{co}} - q'_{\text{co}}, \quad (18)$$

with Δq_{ch} from the earlier definition. For the present RL pairing, $\Delta q_{\text{ch}} = 1$ with $q_{\text{ch}} = 1/2$ and $q'_{\text{ch}} = -1/2$ being

	Polar	A-phase	CSL
Δ_{ia}	$\delta_{i3}\delta_{a3}$	$(\delta_{i1} + i\delta_{i2})\delta_{a3}$	δ_{ia}
\mathbf{n}	$l_{-,3}\hat{\mathbf{e}}_3$	$(l_{-,1} + il_{-,2})\hat{\mathbf{e}}_3$	l_-
Δq_{ch}	1	1	1
Δq_{co}	0	0	-1
g	2	2	0
$\Delta q_{0,\text{co}}$	0	0	2

TABLE I. The order parameter (three-by-three matrix) Δ_{ia} for different transverse phases of the spin-one CSC. With the expression for vector \mathbf{n} for the opposite chirality pairing, defined in Eq. (15), and is shown explicitly in the third row, we compute non-zero eigenvalue $\lambda = \mathbf{n} \cdot \mathbf{n}^*$, and eigenvectors of Eq. (14). Those results then determine the pairing color monopole charge.

the Berry monopole charges associated with \mathbf{A}_R and \mathbf{A}_L , respectively. The color Berry monopole charges q_{co} and q'_{co} can be computed from $\mathbf{A}_{\text{co},mn}$ and $\mathbf{A}'_{\text{co},mn}$ through (6) with averaging by N_λ -fold degenerated states (corresponding to $1/N_\lambda$ factors in Eq. (17)). For later convenience, we record the projected gap matrix (7) below:

$$\tilde{M}_{mn} = c'_{m,a} N_{ab} c_{n,b}. \quad (19)$$

Once the order parameter Δ_{ia} in \mathbf{n} vector is specified, we can evaluate the circulation of velocity and Berry flux according to Eq. (10) explicitly. The relevant expressions for different phases are summarized in Table. I

Topological nodal structure of CSC.— We first discuss the polar phase (see the second column of Table. I). The energy of the quasi-particle excitation $E = \sqrt{k^2 + \Delta_0^2 \lambda}$ is illustrated in Fig. 1 (a), where momentum distribution of the gap is given by $\lambda = \sin^2 \theta$ (see also Refs. [23, 25]). The nodes are at the north ($\theta = 0$) and south poles ($\theta = \pi$). We also find $c_1 = (1, 0, 0)$ and $c_2 = (0, 0, 1)$ which is constant in $\hat{\mathbf{k}}$. Then, Δq is solely given by the spin contribution: $\Delta q = \Delta q_{\text{ch}} = 1$.

The non-zero total velocity circulation implies the obstruction of defining the phase of the gap (7) globally because of the Berry structure of the wavefunction involved in the pairing. To demonstrate this point further, we choose the helicity basis that behaves regularly on the F.S. Near the north pole, we use $\xi_R = (\cos(\theta/2), e^{i\phi} \sin(\theta/2))$ and $\xi_L = (e^{-i\phi} \sin(\theta/2), -\cos(\theta/2))$. The resulting Berry gauge field is also regular at $\theta = 0$: $\mathbf{A}_R = -\mathbf{A}_L = (1 - \cos \theta)/(2k \sin \theta) \hat{\mathbf{e}}_\phi$. Evaluating Eq. (13) explicitly gives

$$\mathbf{l}_\pm = (\cos \theta \cos \phi \pm i \sin \phi, \cos \theta \sin \phi \mp i \cos \phi, \sin \theta), \quad (20)$$

Near the south pole, we need to choose another gauge, e.g., $\xi_R \rightarrow e^{-i\phi} \xi_R$ and $\xi_L \rightarrow e^{i\phi} \xi_L$ and $\mathbf{A}_R = -\mathbf{A}_L = (-1 - \cos \theta)/(2k \sin \theta) \hat{\mathbf{e}}_\phi$ and $\mathbf{l}_\pm \rightarrow e^{\mp 2i\phi} \mathbf{l}_\pm$ also becomes different for Eq. (20). Meanwhile, applying (19) gives $\det(\tilde{M}^\dagger) = l_{+,3}$. Consequently, $\alpha = \phi$ near the north pole and $\alpha = -\phi$ at the south pole. The circulation

around both nodes is dominated by $\nabla_{\mathbf{k}} \alpha$ since \mathbf{A} and \mathbf{A}' are regular and they both equal to 1. Therefore, the sum, coming from the “difference” in α around the nodes that we chose different gauge, is $g = 2 = 2\Delta q$, in agreement with Eq. (10).

Turning to A phase (see the third column of the Table I), the color Berry gauge field also vanishes so $\Delta q = \Delta q_{\text{ch}} = 1$. From the explicitly expression $\lambda = 1 + \cos \theta$, we see that this phase has a single node located at $\theta = \pi$. Using the basis that is regular near the south pole, we find $\det \tilde{M} \propto e^{2i\phi} (1 + \cos \theta)$, indicating $g = 2$. Despite the difference in the number of the nodes and the circulation around the nodes, the relation (10) holds for both the polar and A phases. We note in passing that for the A-phase in LR sector, $\lambda = 1 - \cos \theta$ and hence has a node at the north pole.

The order parameter Δ_{ia} considered here is similar to that of superfluid ^3He . In this nonrelativistic system, the rotation in angular momentum parallels rotation in the color space. The A phase of superfluid ^3He exhibits two topological nodes at south and north poles, each having opposite circulation 1 and -1 which results in a total circulation of zero [27, 32]. Topological nodal structure distinguishes the A-phase of ^3He and transverse CSC.

The Berry structure of the CSL phase contrasts sharply with that of the polar and A phases. It easy to verify that $c_{1,a} \propto \delta_{ai} l_{-,i} = l_{-,a}$ and $c_{2,a} \propto l_{0,a}$ are degenerated eigenmodes of NN^\dagger (16) at $\lambda = 2$ upon using $l_- \cdot l_- = 0$ and $l_- \cdot l_0 = 0$. In fact, since $l_{-,i}$ and $l_{0,i}$ are eigenvectors of the photon helicity operator (see discussion below Eq. (13)), $c_{1,a}$ and $c_{2,a}$ are eigenvectors of “color helicity” operator $\mathbf{J} \cdot \hat{\mathbf{k}}$ with “color” helicity -1 and 0 , which coincide with their color monopole charge. Therefore, $q_{\text{co}} = (-1)/N_\lambda = -1$ with $N_\lambda = 2$ and similarly $q'_{\text{co}} = 1/2$. The color contribution to the pairing of Berry monopoles is $\Delta q_{\text{co}} = -1$ and it precisely cancels that from the chirality $\Delta q_{\text{ch}} = 1$ (see Fig. 1 (b)), implying $g = 0$, which explains the puzzling fact that the CSL phase is fully gapped. Similarly to the CSL phase, one can examine the planar phase $\Delta_{ia} = \delta_{i1}\delta_{a1} + \delta_{i2}\delta_{a2}$, which is fully gapped with $g = 0$.

Gapless excitation.— We now demonstrate that the presence of Δq_{ch} will impose a constraint on the value of the color monopole charge for the gapless excitation of the Bardeen-Cooper-Schrieffer (BCS) state. Those excitations can be expressed in terms of the zero eigenvectors of NN^\dagger and $N^\dagger N$, denoted by c_0 and c'_0 , as follows

$$\phi_{0,R} = \begin{pmatrix} c_0 \otimes \xi_R \\ 0 \end{pmatrix}, \quad \phi'_{0,L} = \begin{pmatrix} 0 \\ c'_0 \otimes \xi_L \end{pmatrix}. \quad (21)$$

The Abelian Berry connection for the gapless mode is given by

$$\mathbf{A}_0 = \mathbf{A}_{0,\text{co}} + \mathbf{A}_R, \quad \mathbf{A}'_0 = \mathbf{A}'_{0,\text{co}} + \mathbf{A}_L, \quad (22)$$

where $\mathbf{A}_{0,\text{co}} = -ic_0^\dagger \nabla_{\mathbf{k}} c_0$ is the color contribution.

Since $c_{0,1,2}$ forms a complete basis in the color space, i.e., $\sum_{\bar{n}=0,1,2} c_{\bar{n},a} c_{\bar{n},b}^* = \delta_{ab}$, we can easily show (see Supplementary Material) $N_\lambda q_{\text{co}} + q_{0,\text{co}} = 0$, where q_{co} are the Berry monopole charges from the degenerated color eigenvectors, $c_{1,2}$. The factor of N_λ appears in the first term since $q_{\lambda,\text{co}}$ is an average of the monopole charge for the $N_\lambda = 2$ degenerate modes. Therefore, $\Delta q_{\text{co}} = -\Delta q_{0,\text{co}}/2$ and $\Delta q = \Delta q_{\text{ch}} - \Delta q_{0,\text{co}}/2$. Rewriting Eq. (10) gives the relation,

$$2\Delta q_{\text{ch}} = g + \Delta q_{0,\text{co}}. \quad (23)$$

The sum rule (23) reveals the rich physical consequence of non-zero Δq_{ch} for the pairing fermions with additional quantum numbers. It implies two general situations:

Scenario A: $2\Delta q_{\text{ch}}$ is saturated by the total circulation g and $q_{0,\text{co}} = 0$.

This situation applies to the polar and A-phase of transverse spin-one CSC (also applies to Refs. [1, 26]). We have checked $c_0 = c'_0 = (0, 0, 1)$ in those cases, corresponding to the blue quark, which does not participate in the pairing. In this case, the system can not be fully gapped.

However, there is another possibility, e.g.,

Scenario B: $2\Delta q_{\text{ch}} = \Delta q_{0,\text{co}}$ and $g = 0$.

For the CSC phase for example, the system is fully gapped ($g = 0$). We find $c_{0,a} \propto l_{+,a}$ and $c'_{0,a} \propto l_{-,a}$ and hence $q_{0,\text{co}} = 1$ and $q'_{0,\text{co}} = -1$ similarly. Therefore, $\Delta q_{0,\text{co}} = 2$ as expected. The gapped excitations $\phi_{0,\text{R}}$ and $\phi'_{0,\text{L}}$ have unusual Berry monopole charges $3/2$ and $-3/2$ as they carry both color helicity (± 1) and spin helicity ($\pm 1/2$).

Longitudinal vs transverse phase.— Let us perform a parallel analysis for the longitudinal phase, say the pairing between right-handed quarks (RR sector). Here, the mean-field Hamiltonian H takes the same form as in Eq. (2) with $\mathcal{H}_0 = \boldsymbol{\sigma} \cdot \mathbf{k} - \mu$ and $\mathcal{H}'_{0\text{c}} = \mathcal{H}_0(-\mathbf{k})$ and $M = P_+(\hat{k}_i \Delta_{ia} J_a)$, where σ_i^\perp of (11) is replaced by the longitudinal direction \hat{k}_i . The relevant eigenmodes can be written, $\tilde{\phi} = \tilde{c} \otimes \xi_{\text{R}}$ and $\tilde{\phi}' = \tilde{c}' \otimes \xi_{\text{R}}$ (c.f. Eq (12)). Here, \tilde{c} is the eigenvector of the color matrix $\tilde{N}\tilde{N}^\dagger$ where \tilde{N} is obtained by replacing \mathbf{l}_- in Eq. (15) by \mathbf{l}_0 (note: $(P_+\hat{k})\xi_{\text{R}} = \mathbf{l}_0\xi_{\text{R}}$ where $\mathbf{l}_0 = \hat{k}$). Obviously, $q_{\text{ch}} = q'_{\text{ch}} = 1/2$ and $\Delta q_{\text{ch}} = 0$.

For the A-phase, the color vector $\tilde{c}_{1,2}$ are constant, which results in $q_{\text{co}} = q'_{\text{co}} = 0$, yielding $\Delta q = 0$. The eigenvalue $\lambda = (\hat{\mathbf{k}}_1 + i\hat{\mathbf{k}}_2) \cdot (\hat{\mathbf{k}}_1 - i\hat{\mathbf{k}}_2) = \sin^2 \theta$ has nodes at the north and south pole, where the circulation there are 1 and -1 (the same as the A-phase of ^3He), respectively. Thus, $g = 0$, in accordance with the relation (10). For CSL phase, we confirmed that it is fully gapped ($\lambda = \hat{\mathbf{k}}^2 = 1$) with $\tilde{c}_{1,a} = l_{+,a}$ and $\tilde{c}_{2,a} = l_{-,a}$, which carry opposite ‘‘color helicity,’’ 1 and -1 , respectively, resulting

in $q_{\text{co}} = 0$. We further verify Eq. (23) by noting the zero eigenvector of $\tilde{N}\tilde{N}^\dagger$ is $\tilde{c}_0 = l_0$ that carries zero color Berry flux. So in this phase, the gapless excitation has Berry monopole charge $\pm 1/2$ as q_{ch} instead of $\pm 3/2$ that we found in the transverse CSL phase.

Previously, it was found that the ground state of one-flavor QCD in the non-relativistic limit corresponds to the CSL phase that involves a mixture of the same and opposite chirality pairing [23]. From the standpoint of the Ginzburg-Landau paradigm, such that the symmetry-breaking patterns classify the phases, this supports the continuity connecting the hadronic matter in the low-baryon density and quark matter in the high-density for one-flavor QCD since the symmetry-breaking pattern (CSL) is the same between the non-relativistic and ultrarelativistic limits. However, our studies reveal the consequence of the difference in Berry structure between the same and opposite chirality pairing, offering new insight into the discussion of hadron-quark continuity from the topological perspective.

Summary and outlook.— We have investigated the impact of Berry flux on the BCS state formed by chiral fermions, particularly quarks within one-flavor QCD in the high-density regime. Previous analyses on the topological properties of CSC are mostly concentrated on the CFL phase [33–35]. The rich Berry/topological structure of spin-one CSC was largely unnoticed. Furthermore, we demonstrate that while the transverse and longitudinal CSC phase at a given order parameter share the same global symmetry-breaking pattern, they can be distinguished by the difference in the topological structure of nodes and Berry monopole charge of quasi-particles.

Based on relation (23), we identify two potential scenarios for the pairing between opposite chirality, as discussed in the text. While the analog of scenario A was known in the context of the SC phase of doped Weyl metals [1], scenario B, which is relevant for the CSL phase, has not been recognized to date. The relation (23) can be readily generalized to a class of SC state with chiral quasiparticles carrying other internal degrees of freedom. It is worth noting that the presence of nodal structure would generically lower the condensation energy $\propto \lambda(\hat{\mathbf{k}})$ over the solid angle integration on the F.S. This is precisely why the CSL phase is energetically favorable over the Polar and A-phase. We expect that scenario B is energetically favored in a more general context.

It would be interesting to explore further physical consequences of the gapless modes with unusual Berry monopole charge $\pm 3/2$ in the CSL phase, which exhibits electromagnetic superconductivity [36, 37]. For instance, studying the response to external magnetic/electric fields and quark mass would be valuable. Given the close connection between Berry monopole and quantum anomaly, it may also be worthwhile to investigate the implications of our findings on the criteria for anomaly matching in dense quark matter.

We thank Dima Kharzeev, Zhen Liu, Andreas Schmitt, Naoki Yamamoto, and Ho-Ung Yee for the helpful discussion. This work is supported by the U.S. Department of Energy, Office of Science, Office of Nuclear Physics Award No. DE-FG0201ER41195 (NS). YY acknowledges the support from NSFC under grant No.12175282 and by CUHK-Shenzhen University Development Fund under the Grant No. UDF01003791.

Note added: Proof of $N_\lambda q_{co} + q_{0,co} = 0$

Using $\mathbf{A}_{co,mn} = -ic_m^\dagger \nabla_{\mathbf{k}} c_n$, we compute the non-Abelian Berry curvature ($\partial_i \equiv (\nabla_{\mathbf{k}})_i$ and omitting the color index) :

$$\begin{aligned}
(F_{co,mn})_{ij} &= \partial_i (A_{co,mn})_j - \partial_j (A_{co,mn})_i + i[(A_{co})_i, (A_{co})_j]_{mn} \\
&= -i\partial_i (c_m^\dagger \partial_j c_n) + i\partial_j (c_m^\dagger \partial_i c_n) \\
&\quad - i \sum_{l=1,2} \left[(c_m^\dagger \partial_i c_l)(c_l^\dagger \partial_j c_n) - (c_m^\dagger \partial_j c_l)(c_l^\dagger \partial_i c_n) \right] \\
&= -i(\partial_i c_m^\dagger \partial_j c_n) + i(\partial_j c_m^\dagger \partial_i c_n) \\
&\quad + i \sum_{l=1,2} \left[(\partial_i c_m^\dagger c_l)(c_l^\dagger \partial_j c_n) - (\partial_j c_m^\dagger c_l)(c_l^\dagger \partial_i c_n) \right] \\
&= -i(\partial_i c_m^\dagger \partial_j c_n) + i(\partial_j c_m^\dagger \partial_i c_n) \\
&\quad + i \sum_{\bar{l}=0,1,2} \left[(\partial_i c_m^\dagger c_{\bar{l}})(c_{\bar{l}}^\dagger \partial_j c_n) - (\partial_j c_m^\dagger c_{\bar{l}})(c_{\bar{l}}^\dagger \partial_i c_n) \right] \\
&\quad - i \left[(\partial_i c_m^\dagger c_0)(c_0^\dagger \partial_j c_n) - (\partial_j c_m^\dagger c_0)(c_0^\dagger \partial_i c_n) \right] \\
&= -i \left[(\partial_i c_m^\dagger c_0)(c_0^\dagger \partial_j c_n) - (\partial_j c_m^\dagger c_0)(c_0^\dagger \partial_i c_n) \right], \quad (24)
\end{aligned}$$

where we have used $c_m^\dagger \nabla_{\mathbf{k}} c_n = -(\nabla_{\mathbf{k}} c_m^\dagger) c_n$ and $\sum_{\bar{l}=0,1,2} c_{\bar{l},a} c_{\bar{l},b}^* = \delta_{ab}$. With similar algebra, we compute the trace as

$$\begin{aligned}
\text{tr}(F_{co})_{ij} &= - \sum_{n=1,2} i \left[(\partial_i c_n^\dagger c_0)(c_0^\dagger \partial_j c_n) - (\partial_j c_n^\dagger c_0)(c_0^\dagger \partial_i c_n) \right] \\
&= - \sum_{\bar{n}=0,1,2} i \left[(\partial_i c_{\bar{n}}^\dagger c_0)(c_0^\dagger \partial_j c_{\bar{n}}) - (\partial_j c_{\bar{n}}^\dagger c_0)(c_0^\dagger \partial_i c_{\bar{n}}) \right] \\
&\quad + i \left[(\partial_i c_0^\dagger c_0)(c_0^\dagger \partial_j c_0) - (\partial_j c_0^\dagger c_0)(c_0^\dagger \partial_i c_0) \right] \\
&= - \sum_{\bar{n}=0,1,2} i \left[(c_{\bar{n}}^\dagger \partial_i c_0)(\partial_j c_0^\dagger c_{\bar{n}}) - (c_{\bar{n}}^\dagger \partial_j c_0)(\partial_i c_0^\dagger c_{\bar{n}}) \right] \\
&= \sum_{\bar{n}=0,1,2} i \left[(\partial_i c_0^\dagger c_{\bar{n}})(c_{\bar{n}}^\dagger \partial_j c_0) - (\partial_j c_0^\dagger c_{\bar{n}})(c_{\bar{n}}^\dagger \partial_i c_0) \right] \\
&= i \left[(\partial_i c_0^\dagger \partial_j c_0) - (\partial_j c_0^\dagger \partial_i c_0) \right] \\
&= -F_{0,co}. \quad (25)
\end{aligned}$$

Recalling that q_{co} is an average over degenerated states, ($1/N_\lambda$ factor in (17)), we obtain

$$N_\lambda q_{co} = -q_{0,co}, \quad (26)$$

which was what we wanted.

-
- [1] Y. Li and F. Haldane, Physical Review Letters **120** (2018), 10.1103/physrevlett.120.067003.
 - [2] K. Fukushima, D. E. Kharzeev, and H. J. Warringa, Phys. Rev. D **78**, 074033 (2008).
 - [3] A. Vilenkin, Phys. Rev. D **22**, 3080 (1980).
 - [4] D. T. Son and N. Yamamoto, Phys. Rev. Lett. **109**, 181602 (2012), arXiv:1203.2697 [cond-mat.mes-hall].
 - [5] M. A. Stephanov and Y. Yin, Phys. Rev. Lett. **109**, 162001 (2012), arXiv:1207.0747 [hep-th].
 - [6] S. Jia, S.-Y. Xu, and M. Z. Hasan, Nature Materials **15**, 1140–1144 (2016).
 - [7] Q. Li, D. E. Kharzeev, C. Zhang, Y. Huang, I. Pletikosic, A. V. Fedorov, R. D. Zhong, J. A. Schneeloch, G. D. Gu, and T. Valla, Nature Physics. **12**, 550 (2016), arXiv:1412.6543 [cond-mat.str-el].
 - [8] F. Arnold, C. Shekhar, S.-C. Wu, Y. Sun, R. D. Dos Reis, N. Kumar, M. Naumann, M. O. Ajeesh, M. Schmidt, A. G. Grushin, *et al.*, Nature communications **7**, 11615 (2016).
 - [9] J. Xiong, S. K. Kushwaha, T. Liang, J. W. Krizan, M. Hirschberger, W. Wang, R. J. Cava, and N. P. Ong, Science **350**, 413 (2015), <https://www.science.org/doi/pdf/10.1126/science.aac6089>.
 - [10] X. Huang, L. Zhao, Y. Long, P. Wang, D. Chen, Z. Yang, H. Liang, M. Xue, H. Weng, Z. Fang, X. Dai, and G. Chen, Phys. Rev. X **5**, 031023 (2015).
 - [11] D. E. Kharzeev, J. Liao, and P. Tribedy, (2024), arXiv:2405.05427 [nucl-th].
 - [12] S. Murakami, N. Nagaosa, and S.-C. Zhang, Science **301**, 1348–1351 (2003).
 - [13] S. Y. F. Liu and Y. Yin, Phys. Rev. D **104**, 054043 (2021), arXiv:2006.12421 [nucl-th].
 - [14] B. Fu, L. Pang, H. Song, and Y. Yin, (2022), arXiv:2201.12970 [hep-ph].
 - [15] S. Y. F. Liu and Y. Yin, JHEP **07**, 188 (2021), arXiv:2103.09200 [hep-ph].
 - [16] B. Fu, S. Y. F. Liu, L. Pang, H. Song, and Y. Yin, Phys. Rev. Lett. **127**, 142301 (2021), arXiv:2103.10403 [hep-ph].
 - [17] F. Becattini, M. Buzzegoli, and A. Palermo, Phys. Lett. B **820**, 136519 (2021), arXiv:2103.10917 [nucl-th].
 - [18] F. Becattini, M. Buzzegoli, G. Inghirami, I. Karpenko, and A. Palermo, Phys. Rev. Lett. **127**, 272302 (2021), arXiv:2103.14621 [nucl-th].
 - [19] F. Becattini and M. A. Lisa, Ann. Rev. Nucl. Part. Sci. **70**, 395 (2020), arXiv:2003.03640 [nucl-ex].
 - [20] F. Becattini, (2022), 10.48550/arxiv.2204.01144.
 - [21] M. G. Alford, K. Rajagopal, and F. Wilczek, Nucl. Phys. B **537**, 443 (1999), arXiv:hep-ph/9804403.
 - [22] M. G. Alford, A. Schmitt, K. Rajagopal, and T. Schäfer, Rev. Mod. Phys. **80**, 1455 (2008), arXiv:0709.4635 [hep-ph].
 - [23] T. Schäfer, Phys. Rev. D **62**, 094007 (2000), arXiv:hep-ph/0006034.
 - [24] M. G. Alford, J. A. Bowers, J. M. Cheyne, and G. A. Cowan, Phys. Rev. D **67**, 054018 (2003), arXiv:hep-ph/0210106.

- [25] A. Schmitt, Phys. Rev. D **71**, 054016 (2005), arXiv:nucl-th/0412033.
- [26] S. Murakami and N. Nagaosa, Physical Review Letters **90** (2003), 10.1103/physrevlett.90.057002.
- [27] A. P. Schnyder and P. M. R. Brydon, Journal of Physics: Condensed Matter **27**, 243201 (2015).
- [28] M. Sato and Y. Ando, Reports on Progress in Physics **80**, 076501 (2017).
- [29] F. Wilczek and A. Zee, Phys. Rev. Lett. **52**, 2111 (1984).
- [30] I. Bialynicki-Birula, Progress in optics **36**, 245 (1996).
- [31] N. Yamamoto, Phys. Rev. D **96**, 051902 (2017), arXiv:1702.08886 [hep-th].
- [32] D. Vollhardt and P. Wolfe, *The Superfluid Phases of Helium 3*, Dover Books on Physics Series (Dover Publications, Incorporated, 2013).
- [33] Y. Nishida, Phys. Rev. D **81**, 074004 (2010), arXiv:1001.2555 [hep-ph].
- [34] Y. Hirono and Y. Tanizaki, Phys. Rev. Lett. **122**, 212001 (2019), arXiv:1811.10608 [hep-th].
- [35] M. G. Alford, G. Baym, K. Fukushima, T. Hatsuda, and M. Tachibana, Phys. Rev. D **99**, 036004 (2019), arXiv:1803.05115 [hep-ph].
- [36] A. Schmitt, Q. Wang, and D. H. Rischke, Phys. Rev. Lett. **91**, 242301 (2003), arXiv:nucl-th/0301090.
- [37] B. Feng, D. Hou, H.-c. Ren, and P.-p. Wu, Phys. Rev. Lett. **105**, 042001 (2010), arXiv:0911.4997 [hep-ph].